[Check for updates]

Trueness of 3D printed partial denture frameworks: build orientations and support structure density parameters

Mostafa Omran Hussein[1]*, Lamis Ahmed Hussein[2]

[1]Department of Prosthodontic Sciences, College of Dentistry in Ar Rass, Qassim University, El-Qassim, Saudi Arabia
[2]Dental Biomaterials, Department of Removable Prosthodontics, Faculty of Dentistry, Misr International University, Cairo, Egypt

ORCID

Mostafa Omran Hussein
https://orcid.org/0000-0001-5545-4606

Lamis Ahmed Hussein
https://orcid.org/0000-0001-9001-7559

PURPOSE. The purpose of the study was to assess the influence of build orientations and density of support structures on the trueness of the 3D printed removable partial denture (RPD) frameworks. **MATERIALS AND METHODS.** A maxillary Kennedy class III and mandibular class I casts were 3D scanned and used to design and produce two 3D virtual models of RPD frameworks. Using digital light processing (DLP) 3D printing, 47 RPD frameworks were fabricated at 3 different build orientations (100, 135 and 150-degree angles) and 2 support structure densities. All frameworks were scanned and 3D compared to the original virtual RPD models by metrology software to check 3D deviations quantitatively and qualitatively. The accuracy data were statistically analyzed using one-way ANOVA for build orientation comparison and independent sample t-test for structure density comparison at (α = .05). Points study analysis targeting RPD components and representative color maps were also studied. **RESULTS.** The build orientation of 135-degree angle of the maxillary frameworks showed the lowest deviation at the clasp arms of tooth 26 of the 135-degree angle group. The mandibular frameworks with 150-degree angle build orientation showed the least deviation at the rest on tooth 44 and the arm of the I-bar clasp of tooth 45. No significant difference was seen between different support structure densities. **CONCLUSION.** Build orientation had an influence on the accuracy of the frameworks, especially at a 135-degree angle of maxillary design and 150-degree of mandibular design. The difference in the support's density structure revealed no considerable effect on the accuracy. [J Adv Prosthodont 2022;14:150-61]

KEYWORDS

3D printing; Partial denture; Computer-aided manufacturing; Digital technology; Dimensional measurement accuracy

INTRODUCTION

Fabrication of the removable partial denture (RPD) framework by conventional method is a lengthy process and requires some effort and skills to be

Corresponding author
Mostafa Omran Hussein
Department of Prosthodontic Sciences, College of Dentistry in Ar Rass, Qassim University, 58876, El-Qassim, Saudi Arabia
Tel +966557279282
E-mail m.omran@qu.edu.sa

mastered. These issues could be minimized by the great development in digital dentistry achieved in the last few years. The prototyping manufacturing technology, whether additive or subtractive, offered a good chance to have smoother and facilitated RPD framework fabrication.[1-6] Although additive digital technology is more workable for RPD manufacturing, some technical issues need optimization to gain the desired outcome, besides reducing the printing time and the consumed materials.[2,5,7,8] Selective laser sintering (SLS) is one of the additive technologies that can transfer the virtual RPD frameworks to the final metallic one. Researchers confirmed that SLS is a successful RPD framework manufacturing process and is suitable for clinical application with a mean accuracy level of 97.452 ± 32.575 μm. However, this manufacturing process is still under development, expensive and rarely found in prosthetic laboratories.[5,7,8] Hwang et al.[9] have optimized the SLS printing process and found that the transverse build angle and inter-connected support structure had the best accuracy (167 ± 105 μm) and optimum density, surface roughness, and productivity, compared to the other studying groups. SLS was also appraised in the literature on its ability to manufacture RPD with a range of accuracy (166 ± 9 to 123 ± 9 μm). In contrast, discrepancies were seen at the center of the major connectors.[1,8,9]

Digital light processing (DLP), stereolithography (SLA), and three-dimensional (3D) printing are now the most popular technologies in prosthetic laboratories.[10] They produce RPD frameworks from castable resin with designs virtually created by the dental computer-aided design (CAD) software. Many parameters could affect the accuracy of the 3D printed objects and influence the final results other than the 3D printing technology used.[10-12] One of the main parameters is the layer thickness, which has a great influence on the accuracy.[10,13] Other parameters include build orientations, printing support thickness, support tip sizes and percentage of support density.[14-18] The support structure density is distinguished from the support structure diameters. The support density is the percentage of the number of support structures' surface area and their auxiliary crossing structures generated by the software regardless of the diameter of each support structure. Research has been conducted to study the influence of all these parameters on the accuracy of the crowns, casts, complete denture bases and implant digital surgical guides.[13,15-21]

The International Standards Organization defined trueness (closeness of measured values to the true value) as accuracy (ISO 5725-1).[22] Accuracy in the articles refers to the level of trueness observed between the original 3D object and the scanned objects generated from the 3D printer.[6,11] Many articles applied the reverse engineering and metrology 3D analysis software to precisely detect the quantitative and qualitative 3D deviations between the reference 3D objects and the scanned objects.[19-21] Generally, quantitative analysis was represented as root-mean-square estimate and the qualitative analysis was done by studying and interpreting the color maps generated in the software report representing the surface positive and negative 3D deviations.[13,16,19,20]

We looked for a published article on the influence of different 3D printing parameters on the RPD frameworks generated from castable materials, but no article met the search criteria. Accordingly, the aim of the current research was to study the influence of build orientations and support structure density as 3D printing parameters on the trueness of the RPD frameworks produced by DPL 3D printing technology. The null hypothesis was that there is no influence of the build orientations and support structure density parameters on the accuracy of the RPD frameworks produced by 3D printers.

MATERIALS AND METHODS

Two educational silicone replicas of maxillary Kennedy class III and mandibular Kennedy class I partially edentulous arches were poured by dental stone. Three definite key shapes were drilled on the cast surface at the major connector of the proposed RPD design. The stone casts were 3D scanned at 4 μm accuracy by a desktop 3D scanner (E4; 3Shape, Copenhagen, Denmark) and their 3D models were saved as standard tessellation language (STL) files. Two virtual RPD frameworks were designed on the 3D scanned models by the partial denture module of the dental CAD software (DentalCAD; Exocad Matera v 2.3; Exocad GmbH, Munich, Germany). Framework de-

sign files were exported to be ready for 3D printing as shown in Figure 1. Designed RPD framework files were then imported to a 3D printing software (Chitubox Pro v 1.9; CBD Ltd., Guangdong, China) to manage the 3D printing process and the studied support parameters. Three build orientations (100°, 135° and 150°) and two support structure density (50% and 75%) were selected for this study, as shown in Figure 2.

Sample size calculation was performed using power analysis software (G*Power v3.1.9.4; Heinrich-Heine-Universitat, Dusseldorf, Germany) for build orientation study (Total sample size = 27; effect size [f] = 0.75; actual power = 90%; power = 91%; α = 0.05)

Fig. 1. Maxillary removable partial denture framework design and corresponding STL export seen as (A) and (B), respectively. Mandibular framework design and export seen as (C) and (D).
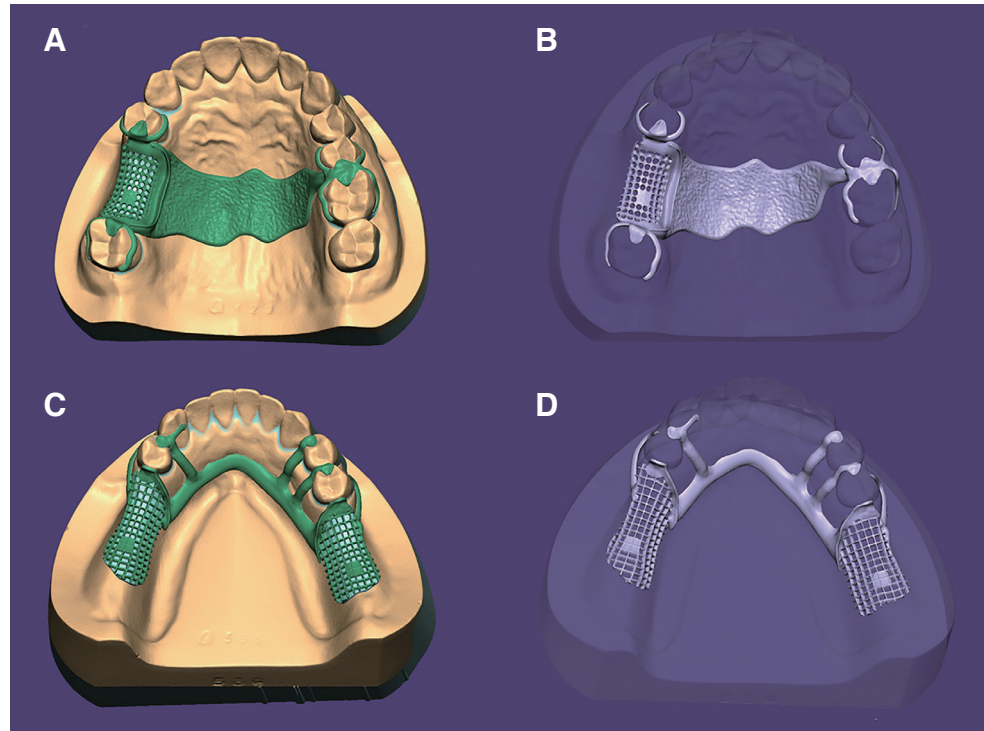

**Fig. 2.** Three-dimensional models of removable partial denture frameworks (blue color) with different build orientations and support structure density after support structure creation (grey color). (A - D) Three-dimensional models of the maxillary removable partial denture frameworks with their support at degree angles 100, 135, 150 and at 75% support structure density, respectively. (E - H) mandibular models with the same sequence.
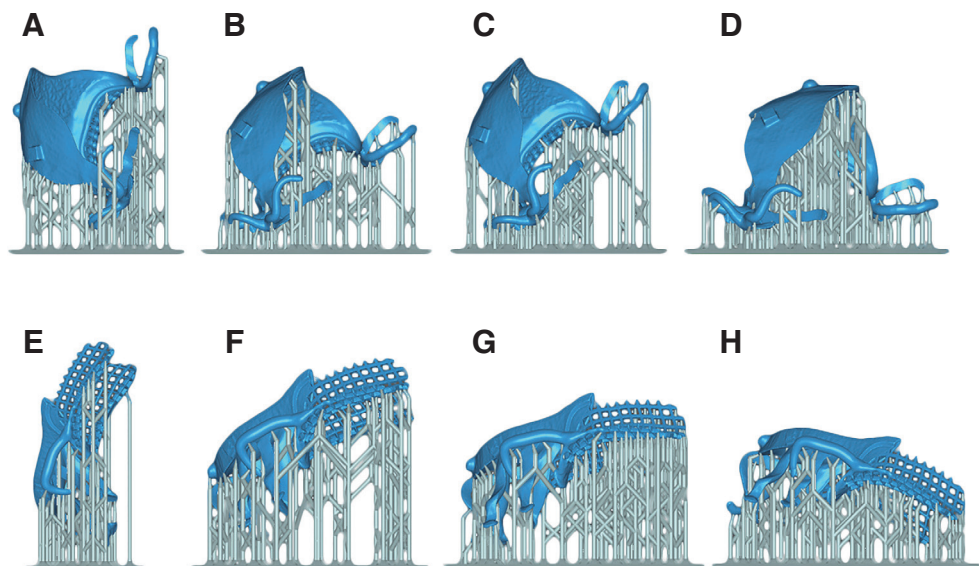
and build structure density study (Total sample size = 20; effect size [f] = 1.6; actual power = 90%; power = 92%; α = 0.05). A total of forty-seven RPD frameworks for each arch were 3D printed (9 for each build angle group and 10 in support density group) from the castable resin (DentaCast; ASIGA, Ann Arbor, MI, USA) using an accurate 3D printer machine (Max UV; ASIGA, Ann Arbor, MI, USA), (Fig. 3).[23] The resin used is an ultraviolet-processed resin, has polymerization range of 385 nm and 405 nm, density of 1.05 - 1.13 g/cm³, hardness of 85 - 88 Shore D, tensile strength of 42.0 MPa, elongation at break of about 10%, and can be used for RPD framework and crown and bridge fabrication. The specification of the 3D printer could be seen in Table 1. This 3D printer is a digital light processing (DLP) type with a pixel resolution of 62 μm and Light-Emitting Diode (LED) wavelength of 385 nm (high power UV LED). The printing speed may reach 50 mm/h. After 3D printing, the 3D resin frameworks

Fig. 3. Removable partial denture frameworks after 3D printing and curing from castable resin and before removal of the support structure.

Table 1. Specification of the digital light processing 3D printer used for frameworks fabrication

Pixel size X, Y	62 μm
Build size X Y, Z	119 × 67 × 75 mm
Light source	385 nm
System size	260 × 380 × 370 mm
File inputs	STL, SLC, STM

were removed, washed in isopropyl alcohol (IPA) for 10 minutes and then dried. Once they were dried, they were post-processed by curing for 20 minutes in the Asiga Flash post-curing chamber (ASIGA, Ann Arbor, MI, USA) to be fully polymerized and get strength to be handled (Fig. 3).

After polymerization, support structures were removed and the resin frameworks were stored in light-proof box until they were 3D scanned. Because the aim of the study was focused on the accuracy of the 3D printed resin framework and avoiding the bias that could evolve from the investing, casting, and finishing and polishing, the manufacturing process was not completed and the processed 3D printed resin was used directly to analyze the trueness of the frameworks.

In order to have better and consistent 3D scanning of the frameworks, they were sprayed by opaque scanning spray (EZ Scan; Alphadent, Waregem, Belgium) with a 3 μm particle size to cover their translucent and reflective nature of the resin. Rubber base index was fabricated to facilitate repeatable position of the frameworks during scanning. After 3D scanning, all files were stored as STL format and labeled according to their group.

Analysis of the frameworks' trueness was performed by comparing the 3D model of the designed framework (reference model) to the 3D models of the scanned samples. A metrology 3D analysis software (Geomagic Control X v 2018.1.1; 3D Systems, Rock Hill, SC, USA) was selected to align, superimpose and measure the difference between the surfaces of the reference model and those of the test model. First, the 3D original reference model and the scanned model were initially aligned by the initial alignment tool; guided by the created key shapes, followed by best fit alignment to ensure accurate surface superimposition and uniform coordinates. The original 3D model was assigned as a reference model and the scanned models were assigned as the test models. By applying 3D compare function, the root-mean-square estimate (RMSE) deviations between the surfaces were calculated from equation

$$\text{RMSE} = \frac{1}{n} \cdot \sqrt{\sum_{i=1}^{n}(x_{1,i} - x_{2,i})^2}$$

where $x1,i$ refers to the measurement point i in the master data, $x2,i$ refers to the measurement point of i in the experimental data, and n refers to the total number of points.[16] Finally, the color map of the deviation was generated. Maximum deviation values of the color scale were set to $\pm$ 300 μm, while the specific tolerance values were set to $\pm$ 50 μm and represented in green color.[1,17,19] Red to yellow color ranges were assigned to the positive section of the color scale while the dark to light blue assigned to the negative values of the color bands. The aforementioned process was repeated between the reference model and all the 3D scanned models of all groups.

RMSE deviation data of all groups were collected and statistically analyzed using statistical analysis software (IBM SPSS Statistics; v 21.0; IBM Corp., Armonk, NY, USA). Data showed normal distribution in both support density and build orientations samples as tested by Shapiro-Wilk test. Accordingly, parametric analysis was considered for checking the difference among the groups (α = .05). The significant difference between the two support density groups in maxillary and mandibular samples was checked by independent sample t-test while one-way ANOVA was used between build orientations groups. Subsequently, Bonferroni post-hoc multiple comparison test with error-adjustment was conducted after checking the homogeneity of variance by levene's test.

In addition to the previous analysis, a point-comparison analysis study was performed to track the deviation of each RPD framework component. A total of forty-eight points of the maxillary framework and thirty-six of the mandibular frameworks were selected. These points encompassed all rests, proximal plates, clasp arms, minor connectors, major connectors, and the finish lines. The mean value and the standard deviation of each component were calculated and tabulated and the color-coded images of the deviated points were generated by the software.

RESULTS

The data generated from the software revealed that mean value of the RMSE of the maxillary frameworks created by 50% support density (0.088 $\pm$ 0.025 mm) was higher than maxillary 75% group (0.068 $\pm$ 0.014 mm). The difference between the two densities was insignificant (P = .134). Values of the mandibular 50% support density group (0.076 $\pm$ 0.010 mm) were higher than 75% density group with no significant difference (P = .757), (Table 2).

The mean of the RMSE of the 100° build orientation of the maxillary frameworks showed the highest value (0.101 $\pm$ 0.010 mm) among the studied build angles, while the 135° angle had the lowest value (0.070 $\pm$ 0.007 mm). There was a significant difference between 135° angle and 100° angle (P = .005). No significance was seen between 150° angle and any other maxillary build angles (Table 3 and Table 4).

Mandibular frameworks showed the highest mean value in the 100° angle group (0.091 $\pm$ 0.006 mm), while 150° angle showed the lowest value (0.066 $\pm$ 0.008 mm). The differences between 150° angle and all other build angles were significant (P < .001). No significant difference was seen between 135° angle and 100° angle (P = .194) (Table 3 and Table 4).

The color maps of the 100° and 150° maxillary RPD frameworks revealed areas of negative deviation represented as grades of dark to light blue colors concentrated at the periphery of the mid-palatal major

Table 2. Descriptive statistical values (mm) and independent sample t-test of the maxillary and mandibular frameworks printed by different support density settings

	Mean	SD	t-value	Sig. (2-tailed)	Significance
50% Maxillary	0.088	$\pm$ 0.025	1.673	.134	NS
75% Maxillary	0.068	$\pm$ 0.014			
50% Mandibular	0.076	$\pm$ 0.010	0.317	.757	NS
75% Mandibular	0.075	$\pm$ 0.004			

NS; not significant.

Table 3. Descriptive statistical values (mm) and ANOVA test between different build orientation groups in both maxillary and mandibular frameworks

Build angle groups	Mean	SD	F-value	Sig.
angle 150 Maxillary	0.083	± 0.020		
angle 135 Maxillary	0.070	± 0.007	7.447	.006[a]
angle 100 Maxillary	0.101	± 0.010		
angle 150 Mandibular	0.066	± 0.008		
angle 135 Mandibular	0.083	± 0.005	19.866	.000[b]
angle 100 Mandibular	0.091	± 0.006		

[a, b] significant at $P < .05$

Table 4. Bonferroni Post-hoc test for multiple comparisons with adjustment for different build orientation groups in both maxillary and mandibular frameworks

Comparison of mean difference	Mean difference	P-value	Significance
Max 150 v 135	0.0125	.418	NS
Max 150 v 100	-0.0183	.114	NS
Max 135 v 100	-0.0308	.005	Significant
Mand 150 v 135	-0.0174	.002	Significant
Mand 150 v 100	-0.0258	.000	Significant
Mand 135 v 100	-0.0083	.194	NS

NS; not significant. Max; maxillary. Mand; mandibular.

connectors. The color map of the 135° angle group showed more homogenous and lighter color than other angle groups. Small islands of positive deviation represented in yellow to orange colors were also seen in the minor connectors and finish line areas (Fig. 4). The color map of the 50% support density group showed some islands of positive and negative deviations in the areas of major connector and closer to the minor connector. The color map of the 75% support density group had a slight change from the 50% density group by showing fewer areas of deviation (Fig. 4).

Areas of negative deviation along the lingual bar major connector of the 100° angle were recorded with minimal areas of positive deviation on the minor connectors and the (I-bar) arm. More homogenous deviations were recorded in the 135° and 150° angles with lower deviation values (lighter colors) in the 150° angle (Fig. 5). The middle part of the lingual bar major connector of both 50% and 75% support density groups showed deviation with darker bands in the 50% density group. Some islands of positive devia-

tions could also be seen in the minor connectors of the 50% density group and the lower edge of the lingual bar of the 75% density group (Fig. 5).

Figure 4 color maps generated from metrology software representing different maxillary removable partial denture frameworks build orientations and support density structures. Color band scale seen in right side showing critical values range (+300: -300 μm) with blue color representing negative deviation and red color positive deviation.

In general, as a matter of comparison of point deviations among different build angle groups of the maxillary framework, the 100° angle group had the highest deviation values (0.022 ± 0.012 - 0.175 ± 0.066 mm), while the 135° angle group showed the least deviation values (0.012 ± 0.003 - 0.072 ± 0.017 mm). For the support structure density groups, the 75% group showed less deviation (0.016 ± 0.016 - 0.082 ± 0.007 mm) compared to the 50% group (0.034 ± 0.016 - 0.0911 ± 0.005 mm). Deviation of points on the maxillary framework rests within all studied groups showed higher values on the #14 tooth than all other

Fig. 4. Color maps generated from metrology software representing different maxillary removable partial denture frameworks build orientations and support density structures. Color band scale seen in right side showing critical values range (+300: -300 µm) with blue color representing negative deviation and red color positive deviation.
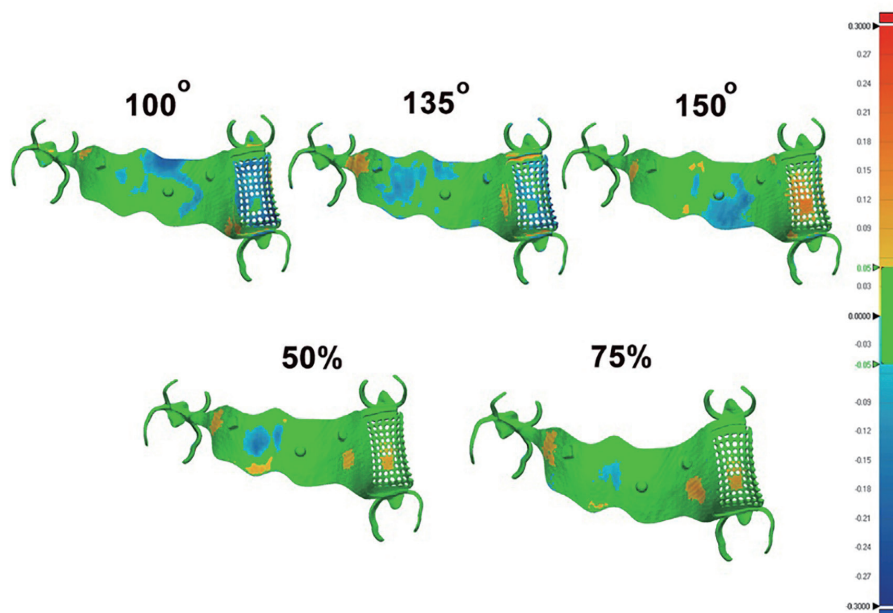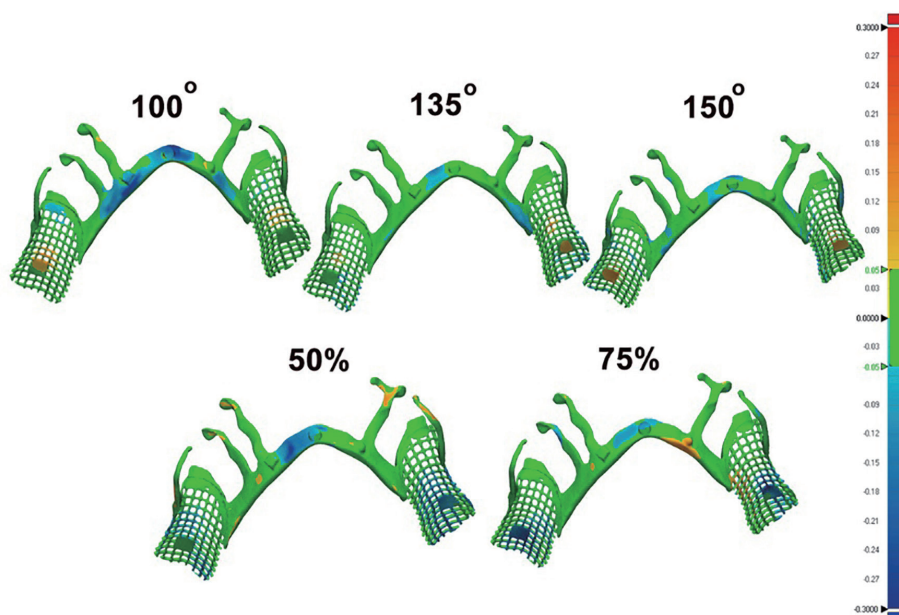

Fig. 5. Color maps generated from metrology software representing different mandibular removable partial denture frameworks build orientations and support density structures. Color band scale seen in the right side showing critical values range (+300: -300 µm) with blue color representing negative deviation and red color positive deviation.

rests, while the rest on the #17 tooth showed the least values (Table 5). For different build angle groups, the tip of the retentive arms of #17 tooth showed higher deviation values, while #26 tooth showed the lowest. Similarly, in support density groups, #17 tooth had higher deviations but #25 tooth showed the lowest value. The highest values of reciprocal arms were recorded in the tip and base of tooth #14 and the lowest values were recorded in the mid-part of tooth #26. The minor connector between teeth #25-26 showed a greater deviation in the area near the connection with the mid-palatal strap. The junction of the proximal plate to the rest seats in tooth #17 showed a higher value compared to the proximal plate of tooth #17. Mostly, the finish line areas showed higher values near the distal part than the mesial one (Fig. 6).

Similar to the maxillary RPD frameworks, the deviation points of the mandibular frameworks revealed an overall higher deviation in the 100° angle group (0.053 ± 0.015 - 0.162 ± 0.032 mm), while the lowest

Table 5. Mean and standard deviation in (mm) of points' deviations of each maxillary RPD framework component

|	100° angle	135° angle	150° angle	50% density	75% density
Rest #25	0.067 ± 0.013	0.035 ± 0.01	0.051 ± 0.02	0.061 ± 0.015	0.03 ± 0.017
Rest #26	0.113 ± 0.025	0.047 ± 0.011	0.063 ± 0.026	0.075 ± 0.032	0.049 ± 0.02
Rest #14	0.132 ± 0.044	0.066 ± 0.019	0.082 ± 0.012	0.0891 ± 0.014	0.061 ± 0.006
Rest #17	0.07 ± 0.006	0.028 ± 0.004	0.044 ± 0.015	0.034 ± 0.016	0.022 ± 0.009
Ret-arm #25	0.053 ± 0.013	0.019 ± 0.007	0.033 ± 0.006	0.0371 ± 0.012	0.016 ± 0.016
Ret-arm #26	0.07 ± 0.006	0.016 ± 0.016	0.03 ± 0.01	0.0381 ± 0.006	0.023 ± 0.008
Ret-arm #14	0.076 ± 0.026	0.021 ± 0.006	0.035 ± 0.013	0.0391 ± 0.007	0.026 ± 0.003
Ret-arm #17	0.089 ± 0.031	0.023 ± 0.004	0.037 ± 0.006	0.047 ± 0.011	0.028 ± 0.005
Rec-arm #25	0.089 ± 0.036	0.029 ± 0.005	0.043 ± 0.012	0.053 ± 0.01	0.024 ± 0.004
Rec-arm #26	0.022 ± 0.012	0.012 ± 0.003	0.026 ± 0.01	0.036 ± 0.007	0.031 ± 0.011
Rec-arm #14	0.081 ± 0.046	0.037 ± 0.016	0.051 ± 0.002	0.0561 ± 0.011	0.042 ± 0.012
Rec-arm #17	0.06 ± 0.015	0.026 ± 0.004	0.044 ± 0.008	0.054 ± 0.003	0.051 ± 0.005
Minor-c #25-26	0.175 ± 0.066	0.058 ± 0.017	0.075 ± 0.008	0.0841 ± 0.019	0.053 ± 0.015
Proximal-p #14	0.054 ± 0.016	0.024 ± 0.008	0.038 ± 0.006	0.05 ± 0.011	0.036 ± 0.01
Proximal-p #17	0.058 ± 0.012	0.028 ± 0.015	0.042 ± 0.016	0.0481 ± 0.012	0.055 ± 0.006
Major-c	0.124 ± 0.026	0.072 ± 0.017	0.084 ± 0.018	0.0911 ± 0.005	0.082 ± 0.007
Finish-L	0.143 ± 0.042	0.059 ± 0.008	0.073 ± 0.013	0.083 ± 0.022	0.075 ± 0.016

c = connector, p = plate, L = line.
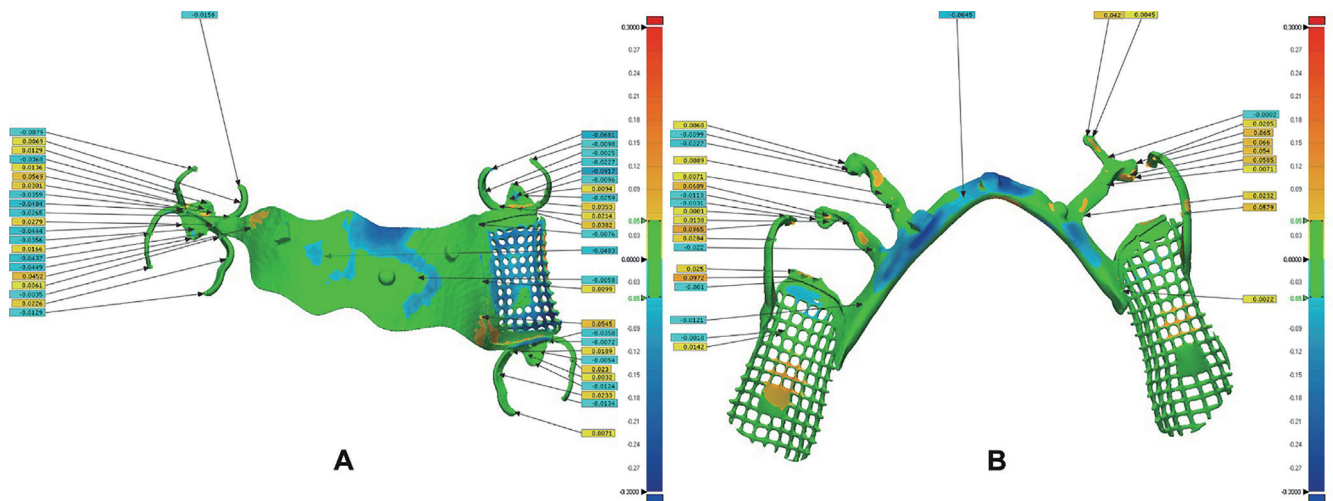
Fig. 6. Sample of the color map of points' deviation analysis of each component of the maxillary and mandibular frameworks seen in (A), (B) images, respectively.

values were in the 150° angle group (0.022 ± 0.007 - 0.075 ± 0.006 mm). The overall points' deviation of the components of the 50% density group was higher than the 75% density group except for the rest of tooth #44 (Table 6). The cingulum rest on tooth #33 revealed the highest deviation among all other rests, while the lowest deviation was in the rest of #44 tooth of group 150° angle. Similarly, the occlusal rest on tooth #44 of group 75% density showed the least deviation of all rests compared to the 50% density group. Although the tip of the I-bar arm of tooth #34 showed a higher value for all build angle groups, the arm on tooth #45 had the higher deviation in the structure density groups. Among all minor connec-

Table 6. Mean and standard deviation in (mm) of points' deviations of each mandibular RPD framework component

	100° angle	135° angle	150° angle	50% density	75% density
Rest #44	0.053 ± 0.015	0.041 ± 0.013	0.022 ± 0.007	0.036 ± 0.010	0.032 ± 0.006
Rest #45	0.072 ± 0.017	0.058 ± 0.015	0.050 ± 0.013	0.059 ± 0.012	0.057 ± 0.012
Rest #33	0.101 ± 0.024	0.069 ± 0.015	0.061 ± 0.011	0.065 ± 0.014	0.061 ± 0.009
Rest #34	0.055 ± 0.019	0.032 ± 0.010	0.030 ± 0.012	0.035 ± 0.010	0.036 ± 0.008
I-bar-arm #34	0.076 ± 0.014	0.031 ± 0.009	0.032 ± 0.007	0.040 ± 0.018	0.039 ± 0.005
I-bar-arm #45	0.070 ± 0.025	0.030 ± 0.011	0.026 ± 0.006	0.044 ± 0.012	0.040 ± 0.007
Minor-c #33-34	0.066 ± 0.012	0.065 ± 0.015	0.052 ± 0.009	0.060 ± 0.013	0.056 ± 0.010
Minor-c #44	0.064 ± 0.015	0.069 ± 0.008	0.055 ± 0.010	0.057 ± 0.014	0.053 ± 0.012
Minor-c #45	0.080 ± 0.022	0.060 ± 0.005	0.064 ± 0.013	0.066 ± 0.017	0.059 ± 0.008
Proximal-p #34	0.101 ± 0.024	0.077 ± 0.017	0.069 ± 0.007	0.074 ± 0.015	0.069 ± 0.015
Proximal-p #45	0.113 ± 0.017	0.066 ± 0.010	0.075 ± 0.006	0.070 ± 0.008	0.064 ± 0.015
Major-c	0.162 ± 0.032	0.080 ± 0.010	0.073 ± 0.013	0.082 ± 0.012	0.080 ± 0.010
Finish-L	0.091 ± 0.025	0.077 ± 0.020	0.072 ± 0.015	0.076 ± 0.016	0.072 ± 0.017

c = connector, p = plate, L = line.

tors of the mandibular frameworks, the minor connector mesial to tooth #45 showed a higher deviation value, especially at the area between the rest and the junction with the lingual bar. Unlike the other groups, the 135° angle group showed the highest deviation at tooth #44. The proximal plate at tooth #34 had a higher deviation in groups 100° and 150° while the proximal plate at tooth #45 was more deviated in the other groups. Similar to maxillary major connectors, the lingual bar had a higher deviation in the central areas. The lingual finish line showed more deviation at the distolingual ends.

DISCUSSION

The null hypothesis was partially accepted at ($P <$ .05), as there was no significant difference in the accuracy of both maxillary and mandibular RPD frameworks produced with different support structure density. On the other hand, build orientations showed a significant difference in the accuracy of the studied RPD frameworks. Therefore, these results imply that changing the build orientations during 3D printing of the RPD frameworks, produced by DLP 3D printers, could improve the accuracy of the printed frameworks with no such effect recorded with increasing the percentage of the support structure density.

The values reported in the study were within the normal range of previous studies.[1,5,16,17] The results of the study reported that the maxillary RPD frameworks with 135° had the lowest RMSE mean value (0.070 ± 0.007 mm) with a significant difference than the 100° angle mean value. This result confirmed that 135° angle had the best values and therefore the most accurate build orientation among the maxillary build orientations. On the other hand, 150° angle mean value (0.066 ± 0.008 mm) was the lowest among mandibular frameworks, with significant differences. Accordingly, it was the most accurate build orientation among mandibular frameworks. Both the aforementioned findings were confirmed in the color maps as a homogenous distribution with a more dominant green color representing within limit specific tolerance values (± 50 μm) without deviation.[1,17,19]

The design of the DLP 3D printer relied on using UV light at 385 nm wavelength. This high energy power was applied to the printing resin by thousands of micro LEDs source. At a resolution of 62 μm, the photodegradable initiator interacts with light energy to produce reactive free radicals or cations. These, in turn, will trigger the polymerization of light sensitive monomer/oligomer molecules that lead to cross-linking, producing solid material. This process is repeated layer by layer in the z-axis by directing the power source from a downward direction, resulting in a building direction from downward-upward. Accord-

ingly, the first layer generated, which is not totally mature, was subjected to the unpolymerized liquid for a longer time than the last layer. In addition, the effect of gravity may also play a role in the distortion process, which could affect the merging between the generated layers. If the printing time is increased, these shortcomings may increase. This finding agreed with other studies that showed better accuracy with 135° angle and more homogenous deviation color maps.[15,17,19] The middle part of the major connectors was the part most affected by the study parameters, which was a frequent location of areas of deviation. This could be attributed to the distortion that commonly happened at the mid-distance between the right and left parts of the frameworks. Another finding was that most of the negative deviation was in the mid-area, while positive deviation was frequently seen on the sides. This finding coincides with other studies that showed more distortion and negative deviation in the mid-area of the prosthesis.[1,5] It was also observed in the point deviation study that the RPD rests showed a comparable deviation range compared to other studies, especially for group 135° angle of the maxillary framework and 150° angle of the mandibular framework.[1,24] It should be mentioned that these studies used different printing materials and techniques. At the clasp arms, the highest deviation was seen in the tips of the both retentive and reciprocal arms, which match Tasaka *et al*.[24] for the reciprocal arm. However, they recorded a higher deviation in the center of the retentive arm. In the proximal plate areas, the results also matched the previous study by Tasaka *et al*.[24] and were slightly higher than those in the study by Negm *et al*.[1] study. The palatal strap showed a range close to that by Negm *et al*.[1]'s study. In contrast, the lingual bar major connector showed higher deviation values than in the previous study.[24] Generally, we believed that the distribution of these deviations might be attributed to the location and thickness of the printed part. For example, the thicker the component, the more deviation happened as it needed more support structure. It was also due to more shrinkage expected during fusion and more contact with the unpolymerized particles during building. The location of the component may also play a role as the peripheral parts might be more

vulnerable to distortion than others; this confirms the importance of the support structure distribution. However, the RPD framework has complex surface details and variable thickness added to the variations between maxillary and mandibular designs. Thus, the amount and location of deviations could be difficult to be expected and justified. In contrast, the support structure density was believed to have a more potent effect on the resin accuracy because of its role in supporting more object surface area and so was expected to show more accuracy with a higher density group. Surprisingly, no significance was seen in RMSE between these groups, which may be due to an insufficient difference between 50% and 75% support density to show a significant effect.

Unlike the previously discussed process of DLP 3D printing, the final RPD framework was 3D printed from metal powders. This process is called powder bed fusion with the subcategories SLS and SLM, in which the metal powder is subjected to a unified laser beam with a suitable wavelength capable to heat and weld these powder particles together to become a solid piece in the moving bed. Subsequently, heat treatment will be applied in a furnace to assure full fusion between the particles and maintain the required strength.[7,10,25] In such a manner, the SLS process enables avoiding the discrepancies that may happen during investing, casting, finishing and polishing.[7,25]

One of the study limitations was that the 3D printing parameters are not only limited to the build orientations and support density, but some other parameters should also be considered, like support diameter, layer thickness, support structure connection and type of technology used. In addition, the current outcome is in harmony with other outcomes like printing time and amount of materials consumed during printing. Other RPD designs with different classes may also influence the final results.

Based on the aforementioned limitation, the recommendation of the study may include testing other 3D printing parameters on the accuracy, printing time, and materials consumed. Different printing technologies as SLA could also be checked. Moreover, framework fitness and optimization study of the best parameters combination should be studied to have the most feasible outcome in accuracy, printing time,

materials consumed and cost.

CONCLUSION

Three-dimensional printing using DLP technology is an accurate manufacturing process for RPD frameworks. Build orientation had an influence on the accuracy of the frameworks especially at 135-degree angle of maxillary design and 150-degree of mandibular design. The difference in the support's density structure revealed no considerable effect on the accuracy.

REFERENCES

1. Negm EE, Aboutaleb FA, Alam-Eldein AM. Virtual evaluation of the accuracy of fit and trueness in maxillary poly(etheretherketone) removable partial denture frameworks fabricated by direct and indirect CAD/CAM techniques. J Prosthodont 2019;28:804-10.

2. Aarts JM, Choi JJE, Metcalfe S, Bennani V. Influence of build angulation on the mechanical properties of a direct-metal laser-sintered cobalt-chromium used for removable partial denture frameworks. J Prosthet Dent 2021;126:224-30.

3. Xie W, Zheng M, Wang J, Li X. The effect of build orientation on the microstructure and properties of selective laser melting Ti-6Al-4V for removable partial denture clasps. J Prosthet Dent 2020;123:163-72.

4. AlMangour B, Luqman M, Grzesiak D, Al-Harbi H, Ijaz F. Effect of processing parameters on the microstructure and mechanical properties of Co-Cr-Mo alloy fabricated by selective laser melting. Mater Sci Eng A 2020;792:139456.

5. Ahmed N, Abbasi MS, Haider S, Ahmed N, Habib SR, Altamash S, Zafar MS, Alam MK. Fit accuracy of removable partial denture frameworks fabricated with cad/cam, rapid prototyping, and conventional techniques: A systematic review. Biomed Res Int 2021;2021:3194433.

6. No-Cortes J, Ayres AP, Lima JF, Markarian RA, Attard NJ, Cortes ARG. Trueness, 3D deviation, time and cost comparisons between milled and 3d-printed resin single crowns. Eur J Prosthodont Restor Dent 2022;30:107-12.

7. Oropallo W, Piegl LA. Ten challenges in 3D printing. Eng Comput 2016;32:135-48.

8. Hussein MO, Hussein LA. Optimization of digital light processing three-dimensional printing of the removable partial denture frameworks; the role of build angle and support structure diameter. Materials (Basel) 2022;15:2316.

9. Hwang S, An S, Robles U, Rumpf RC. Process parameter optimization for removable partial denture frameworks manufactured by selective laser melting. J Prosthet Dent 2021:S0022-3913(21)00253-5. Online ahead of print.

10. Srinivasan M, Kamnoedboon P, McKenna G, Angst L, Schimmel M, Özcan M, Müller F. CAD-CAM removable complete dentures: A systematic review and meta-analysis of trueness of fit, biocompatibility, mechanical properties, surface characteristics, color stability, time-cost analysis, clinical and patient-reported outcomes. J Dent 2021;113:103777.

11. Unkovskiy A, Schmidt F, Beuer F, Li P, Spintzyk S, Kraemer Fernandez P. Stereolithography vs. Direct light processing for rapid manufacturing of complete denture bases: an in vitro accuracy analysis. J Clin Med 2021;10:1070-81.

12. Ryu JE, Kim YL, Kong HJ, Chang HS, Jung JH. Marginal and internal fit of 3D printed provisional crowns according to build directions. J Adv Prosthodont 2020;12:225-32.

13. Çakmak G, Cuellar AR, Donmez MB, Schimmel M, Abou-Ayash S, Lu WE, Yilmaz B. Effect of printing layer thickness on the trueness and margin quality of 3D-printed interim dental crowns. Appl Sci 2021;11:9246-56.

14. Ravi P, Chen VCP. A focused simulation-based optimization of print time and material usage with respect to orientation, layer height and support settings for multi-pathological anatomical models in inverted vat photopolymerization 3D printing. 3D Print Med 2021;7:1-13.

15. Park GS, Kim SK, Heo SJ, Koak JY, Seo DG. Effects of printing parameters on the fit of implant-supported 3D printing resin prosthetics. Materials (Basel) 2019;12:2533-46.

16. Hada T, Kanazawa M, Iwaki M, Arakida T, Soeda Y, Katheng A, Otake R, Minakuchi S. Effect of printing direction on the accuracy of 3D-printed dentures using stereolithography technology. Materials (Basel) 2020;13:3405-17.

17. Jin MC, Yoon HI, Yeo IS, Kim SH, Han JS. The effect of build angle on the tissue surface adaptation of maxillary and mandibular complete denture bases manufactured by digital light processing. J Prosthet Dent 2020;123:473-82.

18. Alharbi N, Osman RB, Wismeijer D. Factors Influencing the dimensional accuracy of 3D-printed full-coverage dental restorations using stereolithography technology. Int J Prosthodont 2016;29:503-10.

19. Rubayo DD, Phasuk K, Vickery JM, Morton D, Lin WS. Influences of build angle on the accuracy, printing time, and material consumption of additively manufactured surgical templates. J Prosthet Dent 2021;126:658-63.

20. Son K, Son YT, Lee JM, Lee KB. Marginal and internal fit and intaglio surface trueness of interim crowns fabricated from tooth preparation of four finish line locations. Sci Rep 2021;11:13947-57.

21. Rungrojwittayakul O, Kan JY, Shiozaki K, Swamidass RS, Goodacre BJ, Goodacre CJ, Lozada JL. Accuracy of 3D printed models created by two technologies of printers with different designs of model base. J Prosthodont 2020;29:124-8.

22. ISO 5725-1. Accuracy (Trueness and Precision) of measurement methods and results-part 1: general principles and definitions. International Organization of Standardization, (ISO); Germany; Switzerland, 1998.

23. Asiga MAX User Guide. In: https://www.asiga.com/media/main/files/printers/MAX_us_en.pdf., ed 2017. p. 1-2.

24. Tasaka A, Shimizua T, Katoa Y, Okanoa H, Idaa Y, Higuchib S, Yamashitaa S. Accuracy of removable partial denture framework fabricated by casting with a 3D printed pattern and selective laser sintering. J Prosthodont Res 2020;64:224-30.

25. Schweiger J, Edelhoff D, Güth JF. 3D printing in digital prosthetic dentistry: an overview of recent developments in additive manufacturing. J Clin Med 2021;10:2010.